Weinreb and Moses, Brain Stimulation, 2022 - Supplementary

Supplementary methods

1. Neuronal cultures

1.1. Neuronal cultures

Living rat hippocampal neural cultures were prepared according to established protocols [1,2]. Microscope images of an example culture can be seen in Fig. S1. Cultures were used from day in-vitro 14 to 28.

In detail, circular glass coverslips 13 × 0.1 mm (ThermoFisher #0) were cleaned by immersion in 65% nitric acid (Merck 100456) for 2 hours, washed 3 times in DDW, washed 3 times in pure ethanol (Gadot ABS AR), passed through a butane flame, and placed in 24 well plates each ~15.5 mm in diameter and height (ThermoFisher 142475). Coverslips were then coated in PLL by immersion for 24 hours in 1 ml of a filtered solution of 0.01% PLL (Sigma P4707) in 8.5 pH borate buffer [4.75 mg/ml borax (Sigma B9876), 3.1 mg/ml boric acid (Sigma B6768), and 2.5 mM hydrochloric acid (Bio-Lab 32% AR) in DDW]. They were then washed 3 times with 1 ml DDW and incubated for 24 hours in an incubator at 37 °C 5%CO_2 in 1 ml plating medium consisting of MEM+3G solution [MEM medium with no glutamine (Gibco 21090-022) with added 20 µg/ml gentamicin (Sigma G1272), 6 mg/ml glucose (Sigma G5146), and 2 mM GlutaMAX (Gibco 35050-038)] with added 50 µl/ml fetal bovine serum (Gibco 12657-029), 50 µl/ml heat-inactivated donor horse serum (BI 04-124), and 1 µl/ml B-27 Supplement (Gibco 17504).

Pregnant Wistar rats (Envigo HsdHan:WIST) were anesthetized with 0.6 ml of 40 mg/ml (in DDW) intraperitoneal sodium pentobarbital (CTS Chemical Industries Pental) and killed by rapid cervical dislocation. Fetal brains were collected from embryos at embryonic day 19, and hippocampi were dissected out into oxygenated ~4 °C L15+2G solution [L15 medium (Gibco 21083-027) with added 20 µg/ml gentamicin and 6 mg/ml glucose]. Tissues were then incubated for 30 minutes at 37 °C in a papain solution [L15+2G with added 0.2 mg/ml l-cysteine (Sigma C7880), 1 mM $CaCl_2$ (Fluka 21098), 0.5 mM EDTA (Merck 108421), 1.5 mM NaOH (BDH 30731), 1 mg/ml DNase (Sigma DN25), and 0.25 mg/ml papain (Sigma P4762)]. The papain solution was then replaced with a trypsin inhibitor solution [plating medium with added 2.5 mg/ml bovine serum albumin (Sigma A7906) and 2.5 mg/ml trypsin inhibitor (Sigma T6522)]. The trypsin inhibitor solution was then replaced with plating medium, and tissues were dissociated mechanically by repeated trituration through a fire-polished Pasteur pipette.

Dissociated cells were plated on the glass coverslips at 850 × 10^3 cells per well, equating to a density of ~4.5 × 10^3 cells/mm^2. Plates were then stored in an incubator at 37 °C 5%CO_2. The medium was changed 4 days after plating to 1 ml of medium made to block glial proliferation [3] [MEM+3G with added 100 µl/ml heat-inactivated donor horse serum, 20 µg/ml floxuridine (Sigma F0503), and 50 µg/ml uridine (Sigma U3750)]. After an additional 4 days, the medium was changed to 1.5 ml of the final medium [MEM+3G with added 100 µl/ml heat-inactivated donor horse serum]. 0.5 ml of the medium were then replaced every 1-2 days. Resulting cultures are estimated to contain ~10% glial cells [4].

Alternatively, for cultures undergoing viral transfection, a serum "free" medium [Neurobasal medium (Gibco 21103-049) with added 20 µg/ml gentamicin, 2mM GlutaMAX, 12.5 µl/ml fetal bovine serum, and 40 µl/ml B-27] was used instead of the plating medium and final medium. This serum "free" medium with added 20 µg/ml floxuridine and 50 µg/ml uridine was used instead of the medium used to block glial proliferation.

All media were filtered at 0.45 µm before use.

1.2. Calcium imaging

The chemical fluorescent calcium indicator Fluo-4 was used to optically monitor neuronal activity. The genetically encoded indicator GCaMP was used in a single experiment. Intracellular calcium levels (as a proxy for neuronal activity) were characterized by taking the fluorescence intensity, subtracting the mean baseline intensity, and dividing by it (this is designated as ΔF/F) [5]. The imaging medium included 1.5 mM $CaCl_2$ to accurately represent Ca^{2+} concentrations in the cerebrospinal fluid [6], which can significantly affect neuronal excitability [7].

This process is now described in detail. In preparation for imaging with Fluo-4, a culture was removed from incubation and placed into a 35 × 10 mm petri dish (Corning 430165) with 1 ml of 37 °C imaging medium and 4 µl of Fluo-4 solution [1 µg/µl Fluo-4-AM (ThermoFisher F14201) in DMSO]. The dish was then placed in a dark container on an orbital shaker (MRC DOR-2828) at the lowest shaking speed for 1 hour. The medium was then replaced with 2 ml of room temperature imaging medium. After preparation, the culture was kept in the dark until imaging (10-40 min).

Alternatively, where explicitly stated, GCaMP was used. 1 µl/ml of a GCaMP6s [8] AAV9 viral vector solution (≥1 × 10^{13} vg/ml) was added to the culture when the media was changed at day 4 in-vitro. On the day of imaging, the culture was placed into a petri dish with 2 ml 37 °C imaging medium. After preparation, the culture was kept in the dark until imaging (10-40 min). [pAAV.Syn.GCaMP6s.WPRE.SV40 was a gift from Douglas Kim & GENIE Project (Addgene viral prep #100843-AAV9)]

The imaging medium used consisted of 130 mM NaCl (Bio-Lab AR), 45 mM sucrose (J.T.Baker 4072), 10 mM glucose, 10 mM HEPES 1M (Sigma H0887), 4 mM KCl (Merck 104936), 1.5 mM $CaCl_2$ and 1 mM $MgCl_2$ (Sigma M8266) in DDW adjusted to pH 7.4 with 1M NaOH [1].

Imaging was performed using a mercury short-arc light source (Zeiss FluoArc), with a fluorescent filter set comprised of an excitation filter at 455-495 nm (Omega Optical XF1073), a dichroic long-pass filter at 505 nm (XF2010), and an emission filter at 510-560 nm (XF3084). Images were collected using an Electron Multiplying CCD camera (Andor iXon Ultra 897 EMCCD). Illumination intensity was adjusted to prevent visible photobleaching. Imaging was done at an acquisition rate of 8 Hz unless stated otherwise. Fluo-4 is known to have a rise time on the order of a few milliseconds [9], and so an acquisition rate of ~1 kHz (909 Hz) was used in a single experiment where a high temporal resolution was required.

1.3. Network disconnection and pharmacological blockade

Stock solutions of pharmacological agents were prepared ahead of time at ×100 the final target concentration in DDW and stored at -20 °C for no more than 6 months in airtight vials. On the day of the experiment, vials were thawed at room temperature and used only once.

Synaptic transmission blockers were used to disconnect the network: Bicuculline methiodide (Sigma 14343) at a concentration of 40 µM to block $GABA_A$ receptors, CNQX (Sigma C239) at 20 µM to block non-NMDA glutamate receptors, and APV (Sigma A5282) at 20 µM to block NMDA glutamate receptors.

TTX citrate (Alomone Labs T-550) at 1 µM was used to block Na_V channels. RR (Sigma R2751) at 30 µM was used to block TRPA, TRPV, TREK-2, and Piezo type MS channels. GsMTx-4 (Alomone Labs STG-100) at 1 µM was

---

AP, Action Potential; APV, 2-Amino 5-Phosphonopentanoic Acid; CNQX, Cyanquixaline; DDW, Double-Distilled Water; FDM, Fused Deposition Modeling; FOV, Field of View; GABA, Gamma-Aminobutyric Acid; IC50, Half Maximal Inhibitory Concentration; MS, Mechanosensitive; NMDA, N-Methyl-D-Aspartic Acid; NaV, Voltage Gated Sodium; PCD, Passive Cavitation Detection; PET, Polyethylene Terephthalate; PI, Propidium Iodide; PLA, Polylactic Acid; PLL, Poly-L-Lysine; RF, Radio Frequency; ROI, Region of Interest; RR, Ruthenium Red; SD, Standard Deviation; TLC, Thermochromic Liquid Crystal; TTX, Tetrodotoxin; UB, Unstimulated Baseline Activity; US, Ultrasound

used to block Piezo1, TRPC1, TRPC5, and TRPC6 type MS channels. Suramin sodium (AdipoGen AG-CR1-3575) at 100 μM was used to block P2 purinergic receptors.

Following are potency values for these pharmacological agents: Bicuculline $GABA_A$ K_D = 1.2 μM [10]. CNQX AMPA IC_{50} = 0.3 μM, Kainate IC_{50} = 1.5 μM [11]. APV NMDA glutamate receptors K_D = 1.4 μM [12]. TTX Na_V channels $IC_{50} \leq 15$ nM [13]. RR TRPA1 IC_{50} = 3.44 μM, TRPV1 $IC_{50} \leq 1.44$ μM, TRPV5 IC_{50} = 0.121 μM, TRPV6 IC_{50} = 9 μM, TREK-2 IC_{50} = 0.2 μM [14–17]. GsMTx-4 general MS channel K_D = 0.5 μM, Piezo1 K_D = 0.155 μM [18–20]. Suramin P2X IC_{50} = 10.1 μM, $P2Y_{11}$ IC_{50} = 16.2μM, $P2Y_2$ IC_{50} = 47.8 μM [21,22].

1.4. Membrane integrity imaging

PI (Sigma P4170) was used at 5 μM to detect membrane poration. Intracellular fluorescence of PI was compared from before stimulation to 10 minutes after. An increase of over 5% in fluorescence was considered indicative of a compromised membrane.

PI was added to the imaging medium similar to the process described for pharmacological agents. PI imaging was done using a mercury short-arc light source, with a fluorescent filter set comprised of an excitation filter at 503-552 nm (Omega Optical XF1074), a dichroic long-pass filter at 555 nm (XF2017), and an emission filter at 650-690 nm (XF3030). This optical filter set was manually swappable with the optical filter set used for calcium imaging, allowing imaging of the two processes in the same experiment.

2. US neurostimulation

2.1. Generation of US pulses

The acquisition computer controlled a function generator (BK Precision 4079) to emit a sine wave at 500 kHz, which was fed for the desired duration of the US pulse into an RF power amplifier (Industrial Test Equipment Powertron 500 A, Class B, 0 Ω output impedance). The amplifier drove a US transducer (Sonic Concepts H-104, focusing bowl type, 400 W, radius=64 mm, radius of curvature = 63.2 mm) through an impedance matching circuit (Sonic Concepts H-104_NRE, 2Ω). The amplifier output current was monitored using a wideband current monitor coil (Pearson Electronics 2100) connected to an oscilloscope. The oscilloscope was also connected directly to the amplifier output to monitor the output voltage. Fig. S2 shows a schematic of the system architecture.

2.2. Design of the experimental system

The experimental system was designed to minimize the occurrence of acoustic reflections and the formation of standing waves. A schematic of the system can be seen in Fig. 1A.

The US transducer was mounted on one side of the chamber, with the geometric acoustic focus positioned at the center of the culture. Simulations showed that the center of the culture was displaced by 2.7 mm from the area of maximal pressure within the acoustic focus, but since the reduction in pressure was under 10%, we maintained this positioning. US was applied parallel to the culture, from the side. This allows the microscope objective and the air chamber housing it to be positioned at a 90° angle and outside the acoustic path. Also, in this orientation a much smaller cross-section of the culture glass coverslip is projected towards the US source, further minimizing reflections from the coverslip. At the opposite end of the chamber an acoustic absorber (Precision Acoustics AptFlex F28, thickness = 10 mm) was positioned to prevent reflection from the chamber edge. The absorber dissipates ~94% of the incident acoustic pressure at 500 kHz [23].

The design of the system is now described in detail. The water chamber had a tube at the bottom where the microscope objective (Olympus LMPLFLN 10X, working distance = 21 mm) was positioned such that the optical focus was at the center of the culture. At the top of the tube, a circular glass coverslip 25 x 0.2 mm (Deckglaser #2) was glued, which allowed the objective to image the culture through the glass, from outside the chamber. The long working distance of the objective enabled a chamber design that positioned the objective and its tube away from the acoustic focus, minimizing reflections.

The water chamber was mounted on an optical table by two arms extending horizontally out from its sides, attached using thumbscrew clamps to metal posts. This enabled adjustment of the chamber height relative to the microscope such that the focus of the objective was positioned at the center of the culture while ensuring that there was no contact between the objective and the glass coverslip at the top of the tube.

Inside the water chamber, there was a much smaller inner chamber where the culture was located. The inner chamber was suspended from arms that slotted into the external chamber, such that the inner chamber could be easily removed for cleaning between experiments, while its position during the experiment was held constant. As with the objective tube, there was a hole at the bottom of the inner chamber where a circular glass coverslip 13 × 0.15 mm (ThermoFisher #1) was glued to enable imaging of the culture.

In order to allow the passage of US through the inner chamber, the chamber wall oriented towards the transducer, and the one opposite to it, were composed of a 12 μm thick mylar sheet (Jolybar Filmtechnic) glued to the chamber at the edges. Due to the relatively small difference in the acoustic impedances of mylar and water (~3×10^6 and ~1.5×10^6 $kg \cdot s^{-1} \cdot m^{-2}$ respectively) [24] and due to the thickness of the mylar sheet being much smaller than the US wavelength at the frequency used (~5 mm), the sheet was nearly transparent acoustically, with its transmittance calculated to be over 99.99%. Thus, US could pass through without significant reflection. Transmission of US through a thin sheet was calculated using the following formula [25]:

$$D = \frac{1}{\sqrt{1 + \frac{1}{4}\left(\frac{Z_1}{Z_2} - \frac{Z_2}{Z_1}\right)^2 \sin^2 \frac{2\pi d}{\lambda}}}$$

D - transmitted pressure (as a fraction of the incident pressure), Z_1 - acoustic impedance of the surrounding material, Z_2 - acoustic impedance of the sheet material, d - sheet thickness, λ - wavelength in the sheet material.

A separate “forceps” part was used to hold the coverslip with its culture, and to position it within the inner chamber. This part had small grooves that held the coverslip from its edges. The inner chamber was first filled with the imaging medium, and then the “forceps” part with the coverslip was inserted into slots in the inner chamber and lowered into the medium. The culture was thus reproducibly positioned and held at an exact and constant location within the inner chamber. The top of the imaging chamber remained open to allow the introduction of pharmacological agents to the medium. A schematic of how these parts fit together can be seen in Fig. S3.

Solid parts were designed using the FreeCAD parametric modeler software [26] and 3D-printed using an FDM printer (MakerBot Replicator). The water chamber was printed using standard PLA filament. The inner chamber and “forceps” parts were printed using clear, food-safe, PET filament (taulman3D t-glase). This PET filament was used for several reasons. First, since the imaging medium was in direct contact with the inner chamber, a food-safe material was chosen to minimize the entry of unknown chemicals into the medium that could have affected the physiology of the culture. Additionally, PLA was not used because it can leach lactic acid into the medium [27], and lactic acid may affect neuronal physiology [28]. Finally, PET has an acoustic impedance relatively similar to that of water (~1.9×10^6 and ~1.5×10^6 $kg \cdot s^{-1} \cdot m^{-2}$ respectively) [24,29,30] which minimizes the

reflected pressure of US at the water PET boundary. This was calculated to be ~11% of the incident pressure using the following formula [31]:

$$R = \frac{Z_2 - Z_1}{Z_2 + Z_1}$$

R - reflected pressure (as a fraction of the incident pressure), Z - acoustic impedance.

Gluing of the mylar sheets and glass coverslips to the printed parts was done using a medical-grade cyanoacrylate adhesive (Loctite 4011) due to its relatively high resistance to water and fast curing time. Adhesion was aided by using a medical-grade polyolefin primer (Loctite 7701) before applying the adhesive.

2.3. Computational simulation of the experimental system

US simulations were performed using the k-Wave software toolbox [32] for Matlab, which supports the simulation of propagating acoustic waves in heterogeneous media in both 2D and 3D configurations.

For simplicity, and to improve performance, simulations were configured to be linear and lossless. Non-linear distortions increase with frequency and pressure and are minimal at the relatively low frequency and pressure used in this study (~2° phase shift of the peak per cm at 0.5 MHz 1 MPa in water) [33]. Absorption losses are also low for these frequencies (~3.4×10^{-4} dB loss per cm at 0.5 MHz in water) [34].

Running spatially extensive, 3D, high-resolution simulations has very large computational demands. For this reason, the simulations were split into two: lower-resolution simulations were performed over large distances, and then higher-resolution simulations were performed at the focal point, where the higher resolution was required to describe the smaller structures accurately. Pressure measurements from the lower-resolution simulations, at the boundary of the higher-resolution areas, were interpolated and used to describe the source pressures that were then implemented for the higher-resolution simulations.

Low-resolution simulations were run at a spatial resolution of 500 µm, and high-resolution simulations were run at 50 µm. Most simulations were run for a duration of 0.1 ms, corresponding to ~150 mm of distance traveled by the acoustic wave.

The simulated space was first designed in FreeCAD using the same models from the experimental system design. 3D models were exported from FreeCAD as STL files and then converted to voxel volumes using the Mesh Voxelisation software package [35] for Matlab. These voxel volumes were then used to define the material properties of the simulation space in k-Wave.

Simulations were configured with the following material properties (speed of sound, density): water - 1497 m/s, 999 kg/m^3; air - 346 m/s, 1.184 kg/m^3; glass - 5640 m/s, 2230 kg/m^3. [36]

2.4. Verification of the experimental system

The pressure output from the transducer was measured using a calibrated hydrophone (Onda HNR-0500) placed at the acoustic focus in a large water tank. The relation between the voltage at the output of the function generator, as set by the computer, and the actual pressure of the US pulse generated by the transducer was linear over the entire applicable range.

The actual duration of the extremely short stimulation pulse (2 cycles of 2 µs duration each) was verified using the hydrophone in a large water tank. The pulse duration at -6 dB was 3.96 µs, and the pulse duration at -20 dB was 11.04 µs. This confirmed that there was no prolonged ringing in the transducer, and that the pulse indeed diminished very rapidly.

Reflections in the experimental system were examined using the hydrophone positioned ~1 mm above the center of the face of the culture glass, within the experimental chamber. Reflections to pulses of duration in all the range used, from 4 µs to 40 ms, were below 10% of the pulse amplitude, and diminished to under 1% within 0.5 ms after the pulse. The hydrophone measurement for 4 µs pulses is shown in Fig. S4. The presence of the hydrophone in the chamber can itself generate reflections, and thus during the actual experiments reflections are probably even weaker.

The location and size of the US focus were examined using a TLC sheet (SFXC R25C5W). The TLC sheet was positioned vertically at the location of the culture, with the culture glass removed, within the experimental chamber (Fig. S5A). Fig. S5B shows the response of the sheet to repeated 100 ms US pulses, with pronounced color changes indicating the location of the US focus, in good correspondence with the simulated focus localization.

2.5. US pulse parameters

All US pulses used in this study were single pulses with a fundamental frequency of 500 kHz.

Repeated stimulation of connected cultures (*'Single US pulses stimulated fully connected neuronal cultures'* Section, Fig. 2A) used a pulse duration of 40 µs, a peak pressure of 0.67 MPa, and a 15 min interval between pulses.

For disconnected cultures, both with and without TTX (*'Single US pulses stimulated pharmacologically disconnected neurons'* and *'AP blockade abolished the response to US'* Sections, Fig. 2B-E), a pulse duration of 40 ms and a peak pressure of 0.35 MPa was used. To avoid attrition effects, only the first pulse applied to each culture was used in the analysis.

Membrane poration assays (*'US stimulation was not associated with membrane poration'* Section, Fig. 3) used pulse durations of 4 µs and 40 ms, and a peak pressure of 0.35 MPa. The example shown in Fig. 3 is from a 4 µs pulse. Again, only the first pulse applied to each culture was taken as the measurement.

Stimulation with extremely short and with standard duration pulses (*'Extremely short US pulses stimulated disconnected neurons'* Section, Fig. 4A,B) used a peak pressure of 0.35 MPa, and again only the first pulse applied to each culture was used. The high sampling rate analysis (Fig. 4C,D) used pulses with peak pressures of 0.35-1 MPa, and the effective stimulations were taken.

Pharmacological blockade experiments (*'P2 receptor blockade did not eliminate the response to US, efficacy increased with pressure'* and *'MS ion channel blockade did not affect the efficacy of US'* Sections, Fig. 5) used a pulse duration of 40 µs. In experiments with suramin (Fig. 5A,B) and with RR (Fig. 5C,D), the first pulse was taken for each culture. Experiments with suramin used a peak pressure of 0.35 MPa or 0.67 MPa. Experiments with RR used a peak pressure of 0.5 MPa. Experiments with GsMTx-4 (Fig. 5E,F) used pulses with peak pressures of 0.5-1.32 MPa, and the first pulse at each increasing pressure was taken.

Attrition experiments with a 25 min recovery time (*'Attrition effects were dominant and occurred at the single-cell level'* Section, Fig. 6A,B) used a pulse duration of 40 µs and a peak pressure of 0.5 MPa. Experiments with a 3-day recovery time (Fig. 6C) used a pulse duration of 40 ms and a peak pressure of 0.35 MPa. The first pulse of the experimental day was taken for each culture. Experiments with repeated stimulation at increasing pressures (Fig. 6D,E) used a pulse duration of 40 ms, peak pressures of 0.35 MPa and 0.67 MPa, and a 2 min interval between pulses, with a second 0.35 MPa pulse given between them.

3. Experimental procedure

The amplifier was initialized and stabilized for 10 minutes with no input and the transducer disconnected. The water chamber with the transducer and absorber was filled with distilled water that was degassed by boiling for 10 minutes, and any remaining bubbles were removed by pipetting. After immersion in water the transducer was connected to the amplifier, and a few

pulses of US were executed to verify the functionality of the system. The inner chamber was rinsed outside of the water chamber in DDW 10 times, before being filled with 8 ml of imaging medium at room temperature. The coverslip with the culture was placed into the inner chamber, which was then placed into the water chamber, which was then covered with aluminum foil to protect from external illumination.

Spontaneous activity was imaged, and the illumination was then turned off to prevent unnecessary photobleaching. Cultures that showed no spontaneous activity were excluded from further testing. Pharmacological agents were first mixed in 1ml of imaging medium and this solution was then added to the culture and gently mixed by pipetting. Illumination and imaging were resumed after a 10 min incubation time.

Illumination was controlled with an automated shutter that was closed between stimulations. The shutter was opened for 15 seconds before and after each stimulation. The voltage and current applied by the amplifier at the transducer were monitored during each stimulation to detect any changes that may indicate disconnections or faults with the system.

We excluded stimulations where cultures showed tearing or separation from the underlying glass. These cultures were not further stimulated.

4. Analysis

4.1. ROI selection

Automatic ROI selection was performed for each culture, using a calcium image sequence of spontaneous activity acquired prior to the pharmacological disconnection of the network. This image sequence was combined with image sequences of the disconnected network acquired during stimulation, and all were taken together and analyzed, searching for spatially contiguous areas of high temporal variance. ROIs were defined as areas that are in the size range expected for neuronal cell bodies (using the CellSort software toolbox for Matlab) [37]. In this manner, only cells that were spontaneously active in the connected network or that became active during the experiment were selected and analyzed. Fluorescence intensity traces for each cell were generated by averaging the intensity of all pixels inside the cell's ROI.

Background ROIs were automatically defined by taking the mean calcium intensity image over the entire experiment and selecting the area of least intensity for each quadrant of that image. An ROI with a similar size to those used for cells was then defined at each such area. A background intensity trace was generated by averaging all the pixels inside all background ROIs together.

An example of the results from this process of ROI selection can be seen in Fig. S6.

4.2. Response detection

For each US stimulation, a time window was taken from 5 seconds before to 10 seconds after the stimulation time point. The fluorescence intensity trace over this time window was taken for each cell's ROI. The intensity trace taken from the background ROIs over this same time window was then subtracted from the cell's ROI intensity trace, thus eliminating global illumination artifacts.

The mean and SD of the trace intensity were taken, and all outlier points (points more than 2 SDs above that mean) were discarded. This process was repeated until no outliers remained. The final mean and SD were then used. The same process was done for the derivative of the intensity [4].

A cell was considered to be responsive to a stimulation if two criteria were satisfied. First, that there was a point within a window of 2 seconds immediately following the stimulation, where the intensity was higher than the intensity at the beginning of the trace plus 3.5 times the intensity SD. Second, that there was a derivative, within that same window, that was bigger than the derivative mean plus the derivative SD. Responses were ignored if the intensity at the end of the trace was more than a single SD below the intensity at the beginning of the trace. [4]

To characterize the unstimulated baseline activity (UB), the same method used to find responses within the time window immediately after the stimulation, was used on the time window immediately before the stimulation. This generated an estimate that included real spontaneous activity, in addition to false positives generated by system noise and the detection method.

4.3. Response characteristics

The amplitude of a response was determined by finding the frame with the maximum intensity within a window of 2 seconds immediately following the stimulation, and then averaging the intensity over 5 frames around this point.

The duration of a response was defined as the time from the initiation of the stimulation to the first frame following the frame with the maximum intensity where the intensity was below 50% of the maximum.

The latency of a response was defined as the time from the initiation of the stimulation to the first frame where the intensity was above 50% of the maximum.

4.4. Statistical tests

Comparisons of the percentage of active cells responsive to stimulation (Figures 2B, 4A, 5A,C,E, 6A) were calculated using the one-sided two-sample t-test method provided in Matlab. Comparison between unstimulated background activities in these figures was calculated using the two-sided method.

Examination of the spatial clustering of responsive cells (*'Single US pulses stimulated pharmacologically disconnected neurons'* Section) was calculated using the one-sided two-sample t-test method provided in Matlab.

Comparisons of mean response characteristics (amplitude, duration, and latency) were calculated using the two-sided two-sample t-test method provided in Matlab.

All tests passed multiple comparison correction using the Benjamini-Hochberg procedure with an FDR of 0.1.

4.5. Figure methods

Boxplot figures (Figures 2B, 4A, 5A,C,E, 6A) were drawn using the IoSR Matlab toolbox [38].

Response trace figures (Figures 2C-E, 4B-D, 5B,D,F, 6B,C,E) were drawn using the shadedErrorBar software package for Matlab [39].

4.6. Temperature calculation

Temperature increases in brain tissue due to US absorption were calculated using the following formulas, which ignore heat loss into the surrounding material [40]:

$$\dot{Q} = \frac{\alpha p_0^2}{\rho c}$$

$$\Delta T = \frac{\dot{Q}\Delta t}{\rho C_p}$$

$\dot{Q}$ - rate of heat generation per unit volume, α - absorption coefficient, p_0 - pressure amplitude, ρ - density, c - speed of sound, ΔT - temperature increase, Δt - US duration, C_p - specific heat capacity.

The following parameter values were used for temperature calculation: absorption coefficient [41] - 1.05 Np·m^{-1} (at 0.5 MHz, with Np the Neper

logarithmic unit), density [42] - 1081 $kg \cdot m^{-3}$, speed of sound [43] - 1510 $m \cdot s^{-1}$, and specific heat capacity [44] - 3640 $J \cdot K^{-1} \cdot kg^{-1}$.

References

[1] Segal M, Manor D. Confocal microscopic imaging of [Ca2+]i in cultured rat hippocampal neurons following exposure to N-methyl-D-aspartate. J Physiol 1992;448:655–76. https://doi.org/10.1113/jphysiol.1992.sp019063.

[2] Papa M, Bundman M, Greenberger V, Segal M. Morphological analysis of dendritic spine development in primary cultures of hippocampal neurons. J Neurosci 1995;15:1–11. https://doi.org/10.1523/JNEUROSCI.15-01-00001.1995.

[3] Segal M. Rat hippocampal neurons in culture: responses to electrical and chemical stimuli. J Neurophysiol 1983;50:1249–64. https://doi.org/10.1152/jn.1983.50.6.1249.

[4] Breskin I, Soriano J, Moses E, Tlusty T. Percolation in living neural networks. Phys Rev Lett 2006;97:188102. https://doi.org/10.1103/PhysRevLett.97.188102.

[5] Smetters D, Majewska A, Yuste R. Detecting action potentials in neuronal populations with calcium imaging. Methods 1999;18:215–21. https://doi.org/10.1006/meth.1999.0774.

[6] Jones HC, Keep RF. Brain fluid calcium concentration and response to acute hypercalcaemia during development in the rat. J Physiol 1988;402:579–93. https://doi.org/10.1113/jphysiol.1988.sp017223.

[7] Penn Y, Segal M, Moses E. Network synchronization in hippocampal neurons. Proc Natl Acad Sci 2016;113:3341–6. https://doi.org/10.1073/pnas.1515105113.

[8] Chen TW, Wardill TJ, Sun Y, Pulver SR, Renninger SL, Baohan A, et al. Ultrasensitive fluorescent proteins for imaging neuronal activity. Nature 2013;499:295–300. https://doi.org/10.1038/nature12354.

[9] Martin P. Fluorescent calcium indicators based on BAPTA. In: Putney JWJ, editor. Calcium Signal. 2nd ed., CRC Press; 2005, p. 2–38.

[10] Hussain S, Bagust J, Gardner CR, Ward RA, Walker RJ. Quantitative analysis of γ-aminobutyric acid (GABA) receptors of purkinje cell layer from rat cerebellar slices. Gen Pharmacol 1990;21:355–64. https://doi.org/10.1016/0306-3623(90)90837-C.

[11] Honore T, Davies SN, Dreier J, Fletcher EJ, Jacobsen P, Lodge D, et al. Quinoxalinediones: Potent competitive Non-NMDA glutamate receptor antagonists. Science (80-) 1988;241:701–3. https://doi.org/10.1126/science.2899909.

[12] Evans RH, Francis AA, Jones AW, Smith DAS, Watkins JC. The effects of a series of omega-phosphonic alpha-carboxylic amino acids on electrically evoked and excitant amino acid-induced responses in isolated spinal cord preparations. Br J Pharmacol 1982;75:65–75. https://doi.org/10.1111/j.1476-5381.1982.tb08758.x.

[13] Goldin AL. Resurgence of sodium channel research. Annu Rev Physiol 2001;63:871–94. https://doi.org/10.1146/annurev.physiol.63.1.871.

[14] Braun G, Lengyel M, Enyedi P, Czirják G. Differential sensitivity of TREK-1, TREK-2 and TRAAK background potassium channels to the polycationic dye ruthenium red. Br J Pharmacol 2015;172:1728–38. https://doi.org/10.1111/bph.13019.

[15] Gavva NR, Klionsky L, Qu Y, Shi L, Tamir R, Edenson S, et al. Molecular determinants of vanilloid sensitivity in TRPV1. J Biol Chem 2004;279:20283–95. https://doi.org/10.1074/jbc.M312577200.

[16] Nagata K, Duggan A, Kumar G, Garcia-Anoveros J. Nociceptor and hair cell transducer properties of TRPA1, a channel for pain and hearing. J Neurosci 2005;25:4052–61. https://doi.org/10.1523/JNEUROSCI.0013-05.2005.

[17] Reichlin S. Transient receptor potential (TRP) channels. In: Flockerzi V, Nilius B, editors. Handb. Exp. Pharmacol., vol. 179, Berlin, Heidelberg: Springer Berlin Heidelberg; 2007, p. 366. https://doi.org/10.1007/978-3-540-34891-7.

[18] Bae C, Sachs F, Gottlieb PA. The mechanosensitive ion channel Piezo1 is inhibited by the peptide GsMTx-4. Biochemistry 2011;50:6295–300. https://doi.org/10.1021/bi200770q.

[19] Bowman CL, Gottlieb PA, Suchyna TM, Murphy YK, Sachs F. Mechanosensitive ion channels and the peptide inhibitor GsMTx-4: history, properties, mechanisms and pharmacology. Toxicon 2007;49:249–70. https://doi.org/10.1016/j.toxicon.2006.09.030.

[20] Gomis A, Soriano S, Belmonte C, Viana F. Hypoosmotic- and pressure-induced membrane stretch activate TRPC5 channels. J Physiol 2008;586:5633–49. https://doi.org/10.1113/jphysiol.2008.161257.

[21] Bültmann R, Starke K. P2-Purinoceptor antagonists discriminate three contraction-mediating receptors for ATP in rat vas deferens. Naunyn Schmiedebergs Arch Pharmacol 1994;350:224. https://doi.org/10.1007/BF00241101.

[22] Jacobson KA, Ivanov AA, de Castro S, Harden TK, Ko H. Development of selective agonists and antagonists of P2Y receptors. Purinergic Signal 2009;5:75–89. https://doi.org/10.1007/s11302-008-9106-2.

[23] Livingstone G, Hurrell A, Morris P, Bell D. Aptflex F28 datasheet. Dorset, UK: 2019. Available from: https://www.acoustics.co.uk/product/aptflex-f28/

[24] Selfridge AR. Approximate material properties in isotropic materials. IEEE Trans Sonics Ultrason 1985;32:381–94. https://doi.org/10.1109/T-SU.1985.31608.

[25] Krautkrämer J, Krautkrämer H. Ultrasonic testing of materials. 2nd ed. Springer; 1990. https://doi.org/10.1007/978-3-662-10680-8.

[26] Riegel J, Mayer W, Havre Y van. FreeCAD. Version 0.15. 2015. Available from: https://www.freecadweb.org/

[27] Conn RE, Kolstad JJ, Borzelleca JF, Dixler DS, Filer LJ, Ladu BN, et al. Safety assessment of polylactide (PLA) for use as a food-contact polymer. Food Chem Toxicol 1995;33:273–83. https://doi.org/10.1016/0278-6915(94)00145-E.

[28] Holmgren CD, Mukhtarov M, Malkov AE, Popova IY, Bregestovski P, Zilberter Y. Energy substrate availability as a determinant of neuronal resting potential, GABA signaling and spontaneous network activity in the neonatal cortex in vitro. J Neurochem 2010;112:900–12. https://doi.org/10.1111/j.1471-4159.2009.06506.x.

[29] taulman3D. MSDS for t-glase (PETT). Saint Peters, MO: 2014. Available from: https://taulman3d.com/uploads/3/4/4/1/34410163/msds_for_t-glase.pdf

[30] Dumbleton JH. Influence of crystallinity and orientation on sonic velocity and birefringence in poly(ethylene terephthalate) fibers. J Polym Sci 1968;6:795–800. https://doi.org/10.1002/pol.1968.160060414.

[31] Kinsler LE, Frey AR, Coppens AB, Sanders J V. Reflection and transmission. Fundam. Acoust. 4th ed., Weinheim: Wiley-VCH; 1999, p. 149–70.

[32] Treeby BE, Cox BT. k-Wave: MATLAB toolbox for the simulation and reconstruction of photoacoustic wave fields. J Biomed Opt 2010;15:021314. https://doi.org/10.1117/1.3360308.

[33] Duck FA. Nonlinear acoustics in diagnostic ultrasound. Ultrasound Med Biol 2002;28:1–18. https://doi.org/10.1016/S0301-5629(01)00463-X.

[34] Hill CR, Bamber JC, Ter Haar GR. Physical principles of medical ultrasonics. 2nd ed. Hoboken, NJ: John Wiley & Sons; 2004. https://doi.org/10.1002/0470093978.

[35] Aitkenhead AH. Mesh voxelisation. Matlab Cent File Exch 2013. Version 1.20.0.0. 2013. Avaliable from: http://www.mathworks.com/matlabcentral/fileexchange/27390-mesh-voxelisation

[36] Rumble JR. CRC handbook of chemistry and physics, 100th edition. 100th ed. CRC Press; 2019.

[37] Mukamel EA, Nimmerjahn A, Schnitzer MJ. Automated analysis of cellular signals from large-scale calcium imaging data. Neuron 2009;63:747–60. https://doi.org/10.1016/j.neuron.2009.08.009.

[38] Hummersone C. IoSR Matlab Toolbox. Software 2017. Version 2.8. 2017. Available from: https://github.com/IoSR-Surrey/MatlabToolbox

[39] Campbell R. shadedErrorBar. Matlab Cent File Exch 2018. Version v1.65.0.0. Available from: https://www.mathworks.com/matlabcentral/fileexchange/26311-raacampbell-shadederrorbar

[40] O'Brien WDJ. Ultrasound–biophysics mechanisms. Prog Biophys Mol Biol 2007;93:212–55. https://doi.org/10.1016/j.pbiomolbio.2006.07.010.

[41] Goss SA, Frizzell LA, Dunn F. Ultrasonic absorption and attenuation in mammalian tissues. Ultrasound Med Biol 1979;5:181–6. https://doi.org/10.1016/0301-5629(79)90086-3.

[42] Barber TW, Brockway JA, Higgins LS. The density of tissues in and about the head. Acta Neurol Scand 1970;46:85–92. https://doi.org/10.1111/j.1600-0404.1970.tb05606.x.

[43] Ludwig GD. The velocity of sound through tissues and the acoustic impedance of tissues. J Acoust Soc Am 1950;22:862–6. https://doi.org/10.1121/1.1906706.

[44] Cooper TE, Trezek GJ. A probe technique for determining the thermal conductivity of tissue. J Heat Transfer 1972;94:133–40. https://doi.org/10.1115/1.3449883.

[45] McLaughlan J, Rivens I, Leighton T, ter Haar G. A study of bubble activity generated in ex vivo tissue by high intensity focused ultrasound. Ultrasound Med Biol 2010;36:1327–44. https://doi.org/10.1016/j.ultrasmedbio.2010.05.011.

Supplementary figures

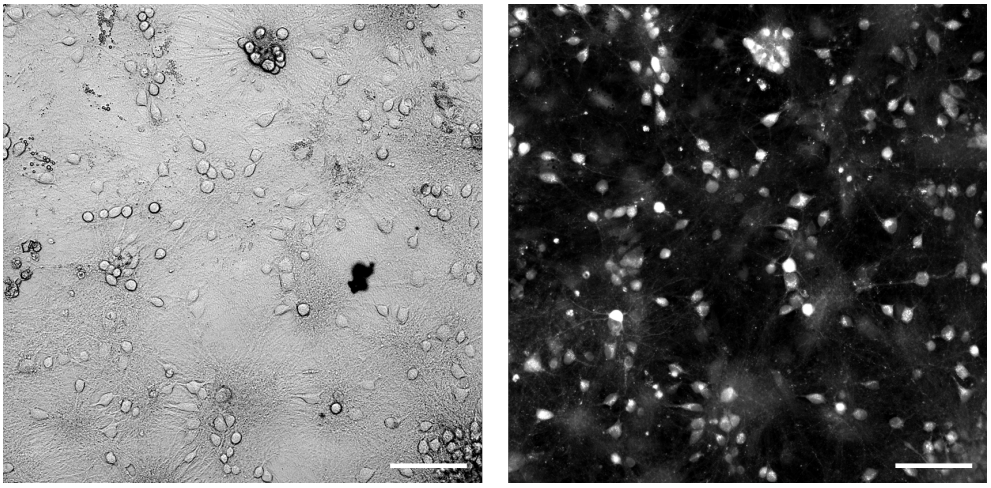

Fig. S1. Primary hippocampal cultures plated on glass - example
Fluorescent and transmitted light imaging of the same FOV from an example rat primary hippocampal culture. Example images were taken 18 days after plating and were acquired with a Leica SP5 confocal microscope using a 10x objective. **Left:** Transmitted light. **Right:** Fluorescent calcium imaging using Fluo-4. Scale bar: 100 µm.

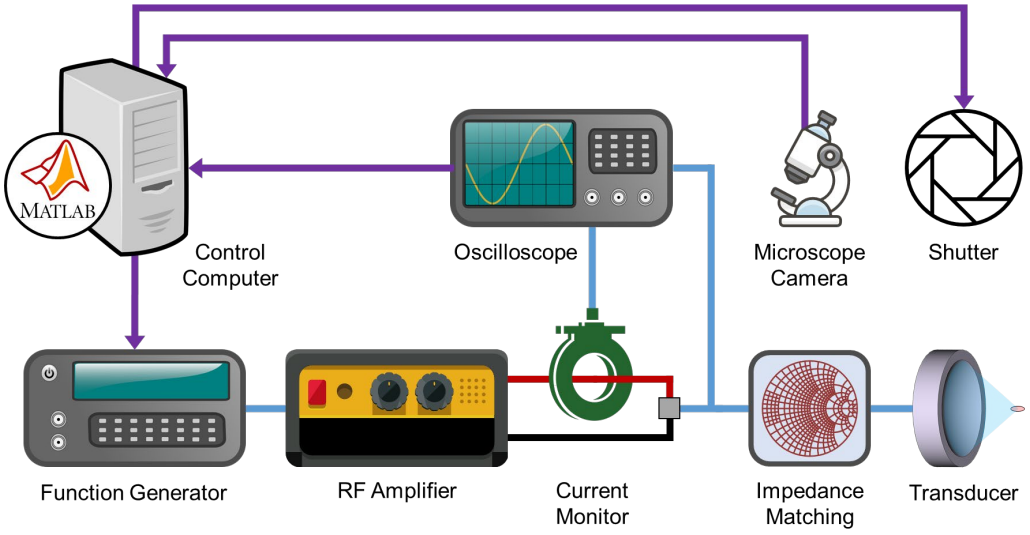

Fig. S2. Experimental system architecture
US pulse generation and microscope imaging were controlled using custom software running on Matlab. US pulses were generated by controlling a function generator, whose output was then amplified, and delivered to the transducer through an impedance matching circuit. Voltage and current running between the amplifier and impedance matching circuit were continuously monitored to verify the functionality of the electronics and the transducer. An automated shutter was closed between stimulations to prevent photobleaching.

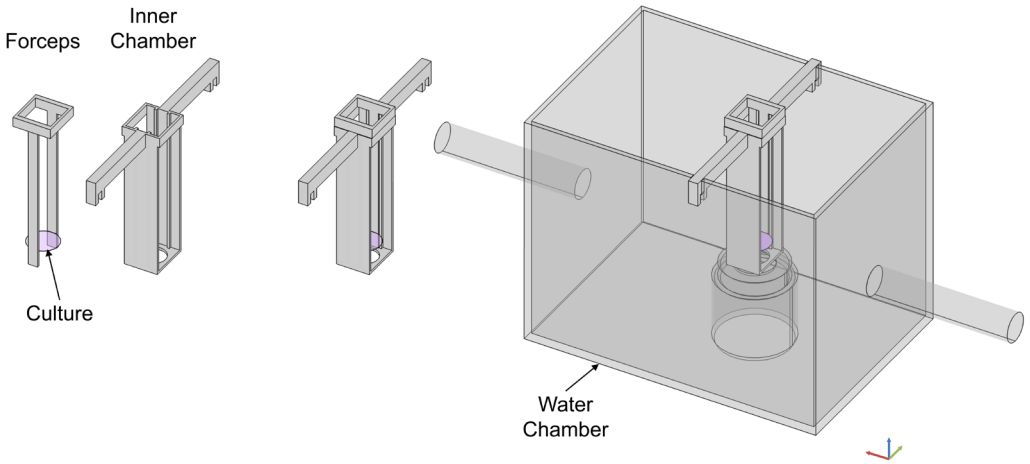

Fig. S3. Culture assembly in experimental chamber

The culture is held from the sides in small grooves in the "forceps" part, which is then slotted into the inner chamber which itself is then positioned into slots in the water chamber. The inner chamber remains open from the top to allow introduction of pharmacological agents to the medium, and contains the imaging medium. The water chamber contains, as its name implies, water. The two sides of the inner chamber, which face towards and away from the US transducer, are comprised of a 12 µm thick acoustically transparent mylar membrane. Cross scale: 10 mm.

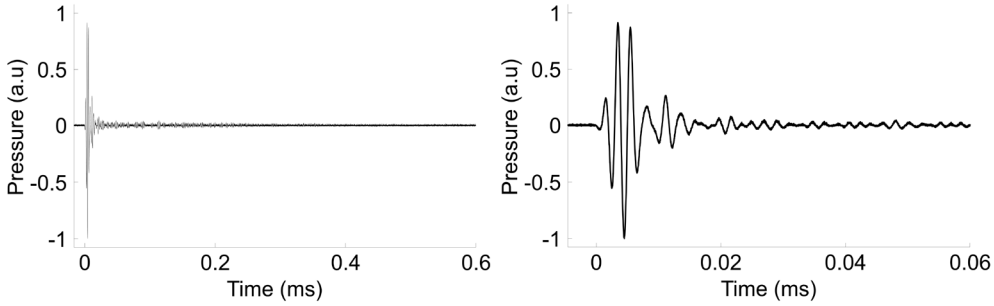

Fig. S4. Hydrophone measurement for 4µs pulses

The hydrophone was positioned ~1mm above the center of the face of the culture glass within the chamber. For 4 µs pulses reflections were found to be minimal, remained below 7% of the pulse amplitude, and diminished to under 1% within 0.3 ms.

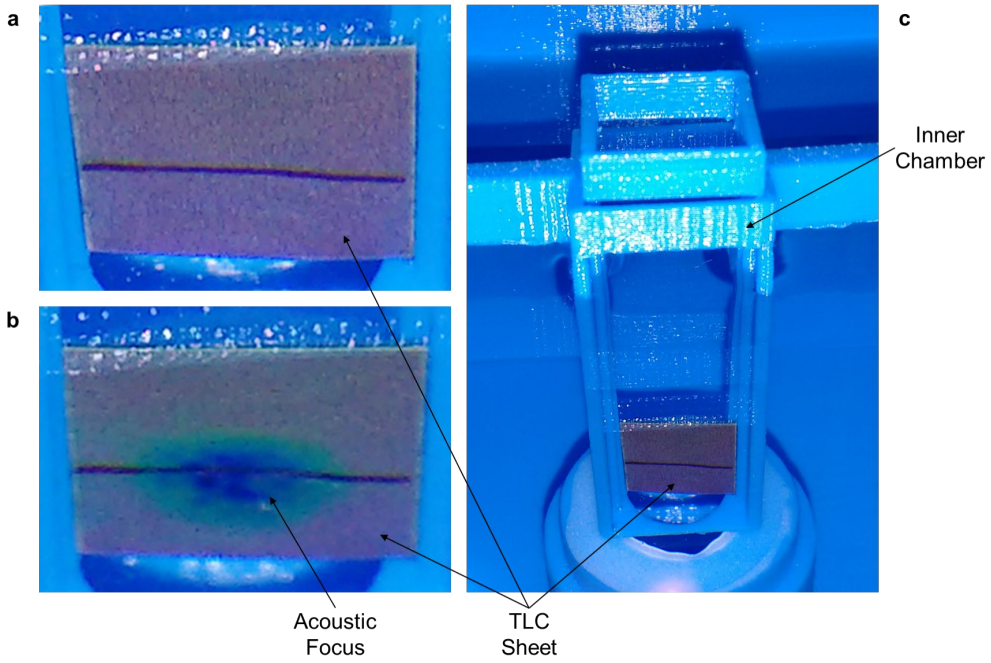

Fig. S5. TLC verification of the ultrasonic focus
A TLC sheet was used to verify the location and size of the US focus. The sheet was placed vertically at the location of the center of the culture. Temperature increases cause the color of the sheet to transition from red to green to blue over a range of 25-30 °C, while changes in pressure have less of a well-defined effect. The horizontal dark line drawn on the center of the sheet marks the position where the culture is normally located. **A:** Zoomed in picture, taken at an angle, of the sheet before application of US pressure. **B:** Same as A, but during repeated 100 ms US pulses. The center of the US focus can be seen in blue. **C:** Zoomed out view of the sheet positioned in the US stimulation system, under water.

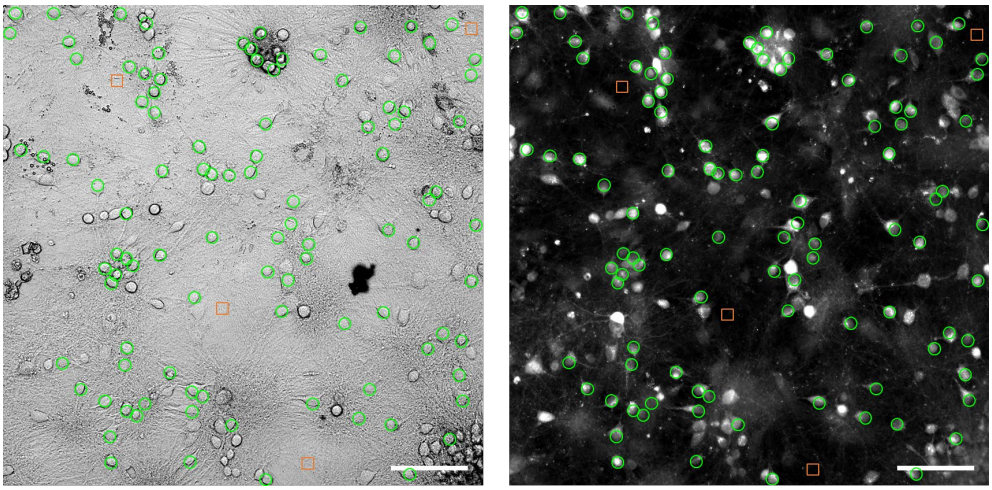

Fig. S6. Cell and background ROI selection - example
Example of automated ROI selection for active cells (green circles) and background (orange squares). Cell ROIs were automatically defined over cell-sized areas of high temporal variance, thus selecting only active cells for analysis. Background ROIs were automatically defined over areas of lowest brightness. **Left:** Transmitted light. **Right:** Fluorescent calcium imaging using Fluo-4. Scale bar: 100 µm.

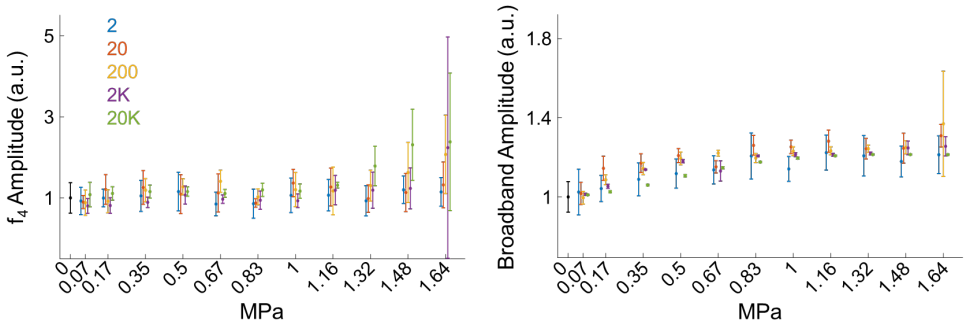

Fig. S7. Analysis of hydrophone voltage during US using passive cavitation detection (PCD)
The hydrophone was placed within the inner chamber, immersed in imaging media, ~1 mm above the center of the face of a culture. PCD was performed according to McLaughlan et al. (2010) [45]. Shown is the peak of the spectra at the 4th harmonic of the US frequency (mean±SD, left), and the sum over the broadband noise regions of the spectra (mean±SD, right). Broadband regions were defined as the spectra above the 4th harmonic without including regions with any further harmonics. Pulses with pressures 0.07-1.64 MPa, and durations 2-20,000 cycles were analyzed. Results were normalized by hydrophone acquisitions with no US applied (0 MPa). n(2 Cycles)=10, n(20, 200, 2K, 20K Cycles)=5 each, n(0 MPa)=31.

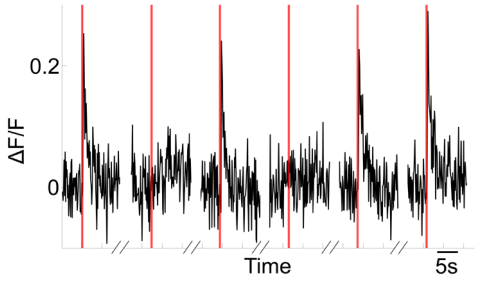

Fig. S8. Example response to repeated stimulations with increasing pressure
Calcium trace from a single cell in a disconnected culture responding to successive stimulations with increasing pressure. Shown are only the first stimulations at each increase in pressure (0.5, 0.67, 0.83, 1, 1.16, and 1.32 MPa). This cell responded to the first 0.5, 0.83, 1.16, and 1.32 MPa stimulations, but did not respond to the first 0.67, and 1 MPa stimulations.

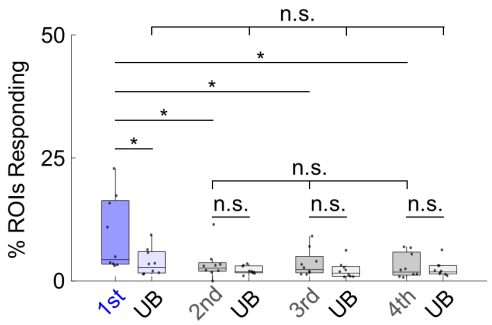

Fig. S9. Response attrition - progression
Percentage of generally active cells responsive to repeated stimulation at a constant pressure, with a 25 min recovery time between pulses, in disconnected cultures. After an initial successful stimulation at the given pressure (1st - 9.5±2.5%, UB=3.9±0.9%), the following three stimulations at the same pressure had a low efficacy, not significantly different from their unstimulated baseline activity (2nd - 3.5±1.1%, UB=2.2±0.3%; 3rd - 3.6±0.9%, UB=2.3±0.6%; 4th - 3.2±0.8%, UB=2.5±0.5%) (mean±SEM, ns=9 each). These three following stimulations also didn't significantly differ in efficacy from each other. UB - unstimulated baseline activity.